

NEURAL REMIXER: LEARNING TO REMIX MUSIC WITH INTERACTIVE CONTROL

Haici Yang¹

Shivani Firodiya¹

Nicholas J. Bryan²

Minje Kim¹

¹ Luddy School of Informatics, Computing, and Engineering, Indiana University, USA

² Adobe Research, San Francisco, CA, USA

minje@indiana.edu

ABSTRACT

The task of manipulating the level and/or effects of individual instruments to recompose a mixture of recording, or remixing, is common across a variety of applications such as music production, audio-visual post-production, podcasts, and more. This process, however, traditionally requires access to individual source recordings, restricting the creative process. To work around this, source separation algorithms can separate a mixture into its respective components. Then, a user can adjust their levels and mix them back together. This two-step approach, however, still suffers from audible artifacts and motivates further work. In this work, we seek to learn to remix music directly. To do this, we propose two neural remixing architectures that extend Conv-TasNet to either remix via a) source estimates directly or b) their latent representations. Both methods leverage a remixing data augmentation scheme as well as a mixture reconstruction loss to achieve an end-to-end separation and remixing process. We evaluate our methods using the Slakh and MUSDB datasets and report both source separation performance and the remixing quality. Our results suggest learning-to-remix significantly outperforms a strong separation baseline, is particularly useful for small changes, and can provide interactive user-controls.

1. INTRODUCTION

Remixing or the task of manipulating the level and/or effects of individual instruments to create a derivative recording is widely used for audio and music production applications such as music content creation (e.g. DJ performances), audio-visual post-production, remastering, podcasting, and more. Music remixing, in particular, is of critical interest and can be used to modify an original version of a song into a different version to suit a specific genre, e.g from country to rock; or to alter the sound stage, e.g., re-position an instrument’s stereophonic location from the center to the left. In addition, there are several *interactive* applications of music remixing. This includes various education scenarios: the learner first wants to *boost* the volume of the guitar solo to familiarize herself to it, then she wants to *suppress* it so that she can play along with the music, but without the guitar solo. Another example could be an amateur band who wants to adjust the level or stereophonic image of all the instruments, while those multiple sound sources are recorded altogether as a single mixture.

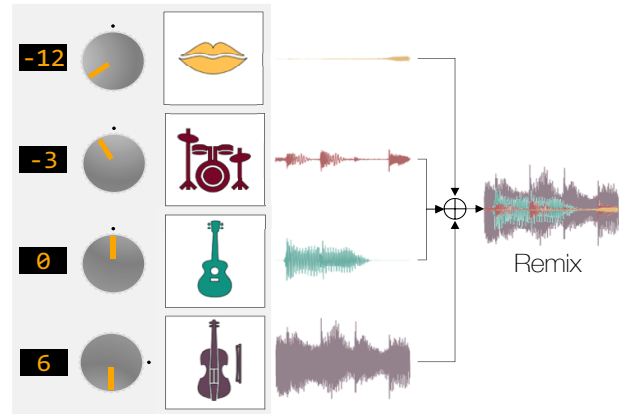


Figure 1: Neural remixing with interactive control.

For these applications and more, separate tracks of the original music are required, which are not always available. So, source separation algorithms are commonly used to estimate individual instrument tracks to allow users to manipulate estimates of separated instruments. Because of this, remixing systems heavily rely on the separation performance and perform well only if a nearly-perfect separation is achieved. Such high-quality results, however, are challenging even for the state-of-art source separation systems, especially when the number of sources becomes large and the separation process is unsupervised [1, 2].

In this work, we aim to minimize separation artifacts found in remixing systems by learning to remix directly. To do so, we first justify our problem formulation with analysis based on commonly used source separation evaluation metrics. Then, we extend a state-of-art source separation model, Conv-TasNet [1], and propose two adaptations toward end-to-end remixing (a) one that applies remixing weights to the source estimates (b) a latent variable control by applying the weights to the bottleneck feature of Conv-TasNet, which is why we chose it as the baseline model. Both of them are regularized, so the separator is informed of the remixing target. We evaluate the proposed methods on two music source separation datasets, Slakh [3] and MUSDB [4] and analyze the behavior of the models on various remixing scenarios.

2. RELATED WORK

In the music information retrieval literature, remixing has been studied from various perspectives, e.g. amplifying single instruments [5, 6], user interface system design [7], and for hearing health [8]. The methodologies in the previous work can be categorized into two kinds: feature-based methods and source separation-based methods. When aiming at adjusting one or a limited number of specific musical instruments among others (usually drums), remix often relies on the feature of the target sources. Yoshii et al. apply template matching to localize the single tone of drum in the polyphonic music and to detect its onset and offset, aiming to adjust the volume and timbre of drum and bass sources [6]. Similarly, in [5] band-wise harmonic/noise decomposition utilizes the stochastic part of the signal in different frequency bands to detect drum events. Those drum-specific remixing systems report successful performance in both attenuation (-10 and -6 dB) and amplification (10 dB) tasks. However, its application on limited instruments is an obvious downside. Therefore, the multi-source control scenario necessitates another methodology—remixing based on music source separation (MSS).

When a remixing system uses estimated sources, it inevitably suffers from the imperfect separation quality (will be discussed in detail in Sec. 3.1). In earlier years, side information was often provided to aid the less powerful separation models. Woodruff et al. proposed a remixing system that works with stereophonic signals [9]. They define an informed sources separation system which makes use of the knowledge of spatial information and scores to assist the separation decision. Itoyama et al. describe a user interface system for music remixing, where the MSS step integrates harmonic and inharmonic models, and relies on synchronized MIDI files [10].

The MSS performance has increased significantly, since deep learning was introduced in the field. By utilizing the deep neural network’s capability of learning complex representation, researchers have explored a variety of methods and architectures for MSS, such as joint optimization of masks and recurrent neural networks [11], network blending [12], unsupervised learning [13], and manipulation of latent variables [14, 15]. Compared to conventional signal processing methods, deep learning also shows its strength in waveform-domain processing [16–18] which to the most extent preserves the phase information. Recent research shows a trend to take account more auxiliary information, e.g., musicology [19] or content information [20]. Open-Unmix nicely summarizes various open-source MSS implementations [21].

The advancements in deep learning-based MSS also influences the research on remixing [7, 8]. In [22] an evaluation mechanism is proposed to investigate the influence of five source separation algorithms on remixing, four of which to some extent involve deep neural networks, either convolutional network or recurrent neural network. The best result reported in this paper is to increase the level of the vocals by up to 6 dB.

It is noticeable that all the remixing systems in the liter-

ature treat source separation and remix as two independent processes, where the remixing serves a post-processor’s role that completely relies on the separation effect. In contrast, our proposed neural remixing systems take mixture signals as input and perform separation and remixing through a single inference pass, which is an end-to-end manner. We claim that this is the first attempt to integrate remixing and source separation in the single model to our best knowledge. Furthermore, it has been shown that manipulating the hidden variables in the neural network provides additional benefits in a source separation system [23]. In this work, we will also investigate the potential of controlling the estimated sources in the latent representations. This kind of interactive system has been proven to be useful in source separation systems [24].

3. METHODOLOGY

3.1 Problem formulation

We argue that the naïve concatenation of the separation and remixing processes is unreasonable for the real-world remixing problem. In a two-source case, for example, we can decompose the recovered source (a vector of time-domain samples) into three components as follows:

$$\hat{\mathbf{s}}_1 = \alpha_1 \mathbf{s}_1 + \beta_1 \mathbf{s}_2 + \mathbf{e}_1, \quad \hat{\mathbf{s}}_2 = \alpha_2 \mathbf{s}_2 + \beta_2 \mathbf{s}_1 + \mathbf{e}_2. \quad (1)$$

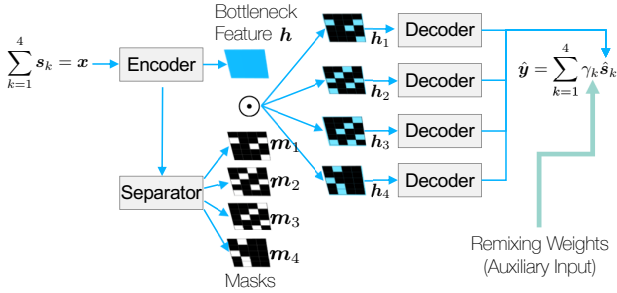
The reconstruction of the first source $\hat{\mathbf{s}}_1$, for example, consists of the scaled ground-truth $\alpha_1 \mathbf{s}_1$, scaled interference $\beta_1 \mathbf{s}_2$, and the artifact generated during the separation process \mathbf{e}_1 . Hence, the perfect scale-invariant separation is achieved when $\beta_1, \beta_2 = 0$ and $\mathbf{e}_1, \mathbf{e}_2 = \mathbf{0}$. This view is commonly used to assess a source separation system, which can decompose the overall distortion, signal-to-distortion ratio (SDR), into the contribution of the other unwanted source, signal-to-interference ratio (SIR), and that of the artifact, signal-to-artifact ratio (SAR) [25].

With a pair of non-negative remixing weights being γ_1 and γ_2 , estimated remix $\hat{\mathbf{y}}$ is derived by,

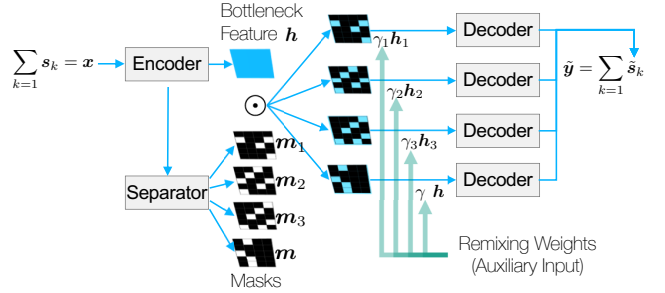
$$\begin{aligned} \hat{\mathbf{y}} &= \gamma_1 \hat{\mathbf{s}}_1 + \gamma_2 \hat{\mathbf{s}}_2 \\ &= (\gamma_1 \alpha_1 + \gamma_2 \beta_2) \mathbf{s}_1 + (\gamma_1 \beta_1 + \gamma_2 \alpha_2) \mathbf{s}_2 \\ &\quad + \gamma_1 \mathbf{e}_1 + \gamma_2 \mathbf{e}_2. \end{aligned} \quad (2)$$

In this rearranged expression, imperfect separation can cause compromised weighting because the approximation $\gamma_1 \approx \gamma_1 \alpha_1 + \gamma_2 \beta_2$ is inaccurate if β_2 is too large or α_1 is too small. Furthermore, even if the separation system completely eliminates the interference, i.e., $\alpha_1, \alpha_2 = 1$ and $\beta_1, \beta_2 = 0$, it could still suffer from the artifacts $\gamma_1 \mathbf{e}_1 + \gamma_2 \mathbf{e}_2$, which is not guaranteed to cancel each other.

One of the answers to this problem is integrating separator and remixer into one model, so both modules’ optimization goals are shared throughout training. Eventually, by informing the separator module of the aims of remixing, it is more apt to recover sources that are suitable for the remixing task. For example, if the separator knows that $\gamma_1 \gg \gamma_2$, it can try harder to suppress \mathbf{e}_1 than \mathbf{e}_2 , because the latter will be suppressed by the small γ_2 value anyway.



(a) The feedforward process for the baseline and *Model-I*.



(b) The feedforward process for *Model-II*.

Figure 2: The neural remixer architectures. Note that the baseline and *Model-I* share the same process during the test time.

3.2 Volume control of multiple sources

In the previous works, the range of the volume adjustment is limited, especially when one wants to boost it. The highest boost level ever reported in the literature that has decent remix quality was 6 dB [22]. Besides, remix for multiple-source (more than 2) cases are under exploration. For example, in [22] and [8], remixing of four-source cases were evaluated, but they treat music as a mixture of vocal and accompaniment, limiting the control only to balance the volume of the lead against the accompaniment track.

Our proposed neural remixing system is trained to cover a wider range of volume change amount from -12 to 12 dB and the number of sources we have experimented is up to five. As a result, our neural remixer can boost or suppress multiple sources per the user’s arbitrary request.

We define the user’s intended volume change amount L as a sound pressure level (SPL) value relative to the original loudness of the reference source s_i mixed in the input:

$$L = 10 \log_{10} \frac{(\gamma_k \mathbf{s}_k)^\top (\gamma_k \mathbf{s}_k)}{\mathbf{s}_k^\top \mathbf{s}_k}, \quad (3)$$

where γ_k denotes the corresponding remixing weights defined in the time domain. For example, the user’s log-based scaling input $L = +10$ dB is converted into $\gamma_k = 3.16$. The ground-truth remix \mathbf{y} is defined as a weighted sum of the ground-truth sources using the source-specific remixing weights, i.e., $\mathbf{y} = \sum_{k=1}^K \gamma_k \mathbf{s}_k$, where K denotes the number of sources. Note that the original mixture is an ordinary sum of the sources with no weighting, i.e., $\mathbf{x} = \sum_{k=1}^K \mathbf{s}_k$. In practice, the system has access only to \mathbf{x} , not to the remixing target \mathbf{y} or any of the sources \mathbf{s}_k .

3.3 The baseline: remixing estimated sources

The baseline utilizes a source separation module that maps the input mixture \mathbf{x} into a set of predicted sources $[\hat{s}_1, \hat{s}_2, \dots, \hat{s}_K]$. We employ Conv-Tasnet-based model that takes a time-domain signal as input and computes the loss in the time domain as well:

$$\mathcal{L}_{\text{BL}} = \sum_{k=1}^K \mathcal{E}(s_k || \hat{s}_k), \quad (4)$$

with an error function $\mathcal{E}(\cdot || \cdot)$, e.g., the sum of squared error or signal-to-noise ratio (SNR). Then, per the user’s input,

the source-specific weights γ_k are applied to the source estimates to approximate the remix with $\hat{\mathbf{y}}$:

$$\mathbf{y} \approx \hat{\mathbf{y}} = \sum_{k=1}^K \gamma_k \hat{s}_k. \quad (5)$$

Note that this process is prone to the inaccurate source control and artifacts as shown in eq. (2). Figure 2a depicts the baseline’s remixing process.

3.4 *Model-I*: the proposed regularization method using the remixing target

The issue we address in the proposed models is that the best-effort source separation system’s performance is imperfect due to the artifact and interference. Our remedy involves the remixing process in training—synthesizing the remix using the recovered sources as in eq. (5), and comparing it to the target remix to update the model parameters. Hence, the *Model-I* loss is with an additional term that penalizes an insufficient remix quality during training:

$$\mathcal{L}_{\text{Model-I}} = \lambda \sum_{k=1}^K \mathcal{E}(s_k || \hat{s}_k) + \psi \mathcal{E}(\mathbf{y} || \hat{\mathbf{y}}), \quad (6)$$

where λ and ψ control the contribution of the source-specific and remix reconstruction losses, respectively. Note that *Model-I* shares the same inference process with the baseline as in Figure 2a, while the proposed regularization improves *Model-I*’s overall separation results for the later use in remixing.

The rationale behind the proposed regularization is to calibrate the optimization results of source separation by imposing a cost on the remix quality. For example, the additional remix reconstruction goal can lead *Model-I* to generating source-specific artifacts e_k that can easily cancel out when they are mixed up, which may not be guaranteed in the baseline. This additional regularizer can also help the system balance the SIR-SAR tradeoff and achieve an optimal remix quality.

3.5 *Model-II*: the proposed control of the latent space

Another proposed approach is to control the loudness of sources in the latent space. Unlike *Model-I* or any other typical remix methods, in *Model-II* we opt to apply the

remixing weights γ_k to one of the network’s hidden layers, instead of source estimates.

Conv-TasNet provides a nice framework in this regard. In Conv-TasNet, the separation is conducted first by computing the bottleneck feature map via the *encoder* module $\mathcal{F}(\cdot)$ and K masks using the *separator* module $\mathcal{G}(\cdot)$,

$$[\mathbf{m}_1, \mathbf{m}_2, \dots, \mathbf{m}_K] \leftarrow \mathcal{G}(\mathbf{x}), \quad \mathbf{h} \leftarrow \mathcal{F}(\mathbf{x}), \quad (7)$$

where the masks are probabilistic, i.e., $\sum_{k=1}^K \mathbf{m}_k = \mathbf{1}$. Then, the bottleneck feature \mathbf{h} is distributed to K different source-specific feature spaces via masking, which are then decoded back into the time-domain reconstruction using the *decoder* module $\mathcal{D}(\cdot)$, respectively:

$$\mathbf{h}_k \leftarrow \mathbf{m}_k \odot \mathbf{h}, \quad \hat{\mathbf{s}}_k \leftarrow \mathcal{D}(\mathbf{h}_k), \quad \forall k, \quad (8)$$

where \odot denotes Hadamard products.

By making use of the separated hidden space, *Model-II* modulates the hidden variables by multiplying their corresponding remixing weights γ_k :

$$\tilde{\mathbf{s}}_k \leftarrow \mathcal{D}(\gamma_k \mathbf{h}_k), \quad (9)$$

of which the output $\tilde{\mathbf{s}}_k$ attempts to reconstruct scaled sources $\gamma_k \mathbf{s}_k$ directly. Along with the remixing regularization we write *Model-II*’s loss as follows:

$$\mathcal{L}_{\text{Model-II}} = \lambda \sum_{k=1}^K \mathcal{E}(\gamma_k \mathbf{s}_k \| \tilde{\mathbf{s}}_k) + \psi \mathcal{E}(\mathbf{y} \| \tilde{\mathbf{y}}), \quad (10)$$

where $\tilde{\mathbf{y}} = \sum_{k=1}^K \tilde{\mathbf{s}}_k$. Multiplying the amplitude-based ratio γ_k to hidden variables does not entail any postulation on the distributions or meanings of the hidden variables. What distinguishes *Model-II* from *Model-I* is the ability of associating the separation behavior with the remix weights, especially during the inference stage. Also, we believe that informing the weights in the earlier step helps the decoder handle any additional artifacts or interference introduced. For example, if the user wants to boost j -th source while suppressing others, $\gamma_j \gg \gamma_k, \forall k \neq j$. Then, *Model-II* can focus more on the precise reconstruction of the dominant source \mathbf{s}_j than the other sources that will be suppressed anyway. Another important corner case is when the remix target is very similar to the input, i.e., $\mathbf{y} \approx \mathbf{x}$ when $\gamma_k \approx 1, \forall k$. In this trivial case, while the baseline still needs to perform source separation and deal with the artifacts, *Model-II* saves the unnecessary separation effort—instead it can just try to minimize the artifact.

4. EXPERIMENT

4.1 Datasets

To validate the merit of the proposed neural remixing methods, we use two music datasets: Slakh [3] and MUSDB [4]. Slakh consists of a large amount of renderings of stem tracks synthesized from MIDI using virtual instruments as well as their mixtures. The tracks belonging to MUSDB, on the contrary, are all professional-level real recordings

	Training	Validation	Test
Slakh	~ 48h	~ 6h	~ 6h
MUSDB	~ 6h	~ 1.25h	~ 1.25h

Table 1: Size of each split data set.

and therefore more close to the real-world scenario. However, the quantity of MUSDB is often not enough to train a large model that generalizes well to the real-world music signals. We first train and test within each dataset independently, then we do cross-database testing, i.e., train the model on Slakh first, then test on MUSDB, and vice versa. In MUSDB, the tracks we use to build up mixtures are vocals, drums, bass, and others. For two-source experiments, for example, the mixture consists of vocals and drums. Similarly, as for Slakh, we test up to five sources in the following order: piano, drums, bass, guitars and string.

4.2 Training setup

We repurposed Asteroid’s Conv-TasNet implementation [26] for our experiments. As the instrument sources composed in the mix are distinctive and we have fixed the order of the sources in our data, we do not consider training with the permutation invariant training (PIT) [27, 28].

We use the entire training set of each dataset for training, and split the original test set into validation and test sets. Eventually, the size of each set is shown in Table 1.

All the waveforms are sampled at 44100 kHz. The model is trained on one-second segments until the validation SDR value does not improve in 50 consecutive epochs. Adam is used as the optimizer with an initial learning rate of 1×10^{-3} [29]. During training, the K remix weights are sampled randomly from the range between -12 to 12 dB and used to form the target remix segments, from which the training and validation loss values.

Note that we substitute the original scale-invariant SDR (SI-SDR) loss function [30] in Conv-TasNet with an ordinary SDR-based one. SI-SDR is insensitive to the scale of the estimated source, thus unsuitable for our problem. Our models make use of SDR’s characteristics of being “scale-variant” to supervise the scale of the estimation.

4.3 Evaluation setup

We evaluate the models by gradually changing the volume of a chosen source. To that end, we define a set of remix weights ranging from -24 to $+24$ dB with a step size of 3 dB, totaling 17 discretized values. The evaluation range is twice wider than the one used for training, in order to test the model’s generalization performance to unseen test environments. To form our evaluation sequence, each set of remix weights only have one source changed and the rest of sources are kept untouched. For each source we examine 16 weight instances, plus the circumstance where none of the sources are adjusted, i.e., 0 dB. We repeat the experiment on all K sources. Per each test example, we test all $16K + 1$ remixing weight combinations. Note that our models are capable of controlling multiple sources at

Train + Test		Baseline		Model-I		Model-II		
		K	$\lambda : \psi = 1 : 0$	$\lambda : \psi = 1 : 1$	$\lambda : \psi = 1 : K$	$\lambda : \psi = 0 : 1$	$\lambda : \psi = 1 : 1$	$\lambda : \psi = 1 : K$
Slakh + Slakh	2	26.34±22.03	22.84±21.28	25.83±22.21	26.94 ±22.81	25.68±21.94	26.33±22.81	25.49±21.58
	3	17.69±16.83	18.69±17.80	18.63±18.05	20.15 ±18.41	18.38±17.64	18.08±17.50	17.56±17.42
	4	5.19±10.14	15.98±12.46	14.94±12.33	15.32±12.43	15.93±12.38	15.07±12.35	16.94 ±12.91
	5	4.16±3.18	11.42±6.29	13.81±8.05	13.11±7.86	11.57±6.39	14.04 ±8.57	13.19±8.28
MUSDB + Slakh	2	21.76±21.35	21.17±22.43	21.14±21.33	22.69±22.80	21.29±22.09	22.00±22.31	23.15 ±22.63
	3	10.96±15.85	12.57±17.32	12.29±17.01	13.65 ±17.79	13.4±17.63	13.32±17.54	13.47±17.76
	4	2.76±9.62	10.93±12.29	11.13±13.29	10.50±12.35	10.89±12.59	11.26 ±13.19	10.59±12.32
MUSDB + MUSDB	2	20.03±10.79	20.61±12.81	20.25±11.20	21.15±13.44	20.73±11.79	20.85±12.50	21.26 ±13.44
	3	13.31±6.63	14.96±9.18	13.84±8.57	15.52±10.11	15.55 ±9.79	15.22±9.55	15.40±10.10
	4	3.01±2.36	12.33±7.18	13.36 ±8.29	11.91±7.14	12.43±7.66	13.30±8.43	11.74±7.04
Slakh + MUSDB	2	15.52±12.83	16.53±11.49	17.15±13.57	17.15±14.33	16.93±13.20	17.80 ±13.68	16.11±13.00
	3	9.76±7.29	11.20±10.84	11.62±10.90	11.86 ±12.10	11.60±10.55	11.76±10.50	11.85±9.95
	4	3.22±2.60	9.43±7.65	10.18 ±7.97	9.95±8.23	9.49±7.78	10.04±7.87	9.92±8.74

Table 2: The mean and standard deviation of SDR (dB) of remix quality.

the same time as they are trained to do so, even though we focus on the potentially most common use case where the user controls only one source of interest.

For the baseline and *Model-I*, all those remixing weight combinations share the same separation results \hat{s}_k , manipulated by γ_k afterwards. For *Model-II*, we run the decoder part several times whenever the remixing weight changes.

In [22] two criteria, sound quality and loudness balance, are suggested to subjectively evaluate the remix. As the evaluation of loudness balance can only be done in a subjective manner, requiring a delicate experimental design and massive trial cases, we opt to assess the models mainly based on the objective remix sound quality. By comparing the recovered remix \hat{y} (the baseline and *Model-I*) or \tilde{y} (*Model-II*) to the ground-truth test remix y . We use SDR, which summarizes the overall reconstruction quality of the remix, and is equivalent to an ordinary SNR in this case. In addition, we compute the SDR, SIR and SAR scores for each estimated source to investigate the impact of remix on the separation behavior.

5. EXPERIMENTAL RESULTS AND DISCUSSION

5.1 Overall remixing performance

Table 2 reports the mean and standard deviation of SDR values of the estimated remix compared to the ground-truth target. Overall, both proposed models achieve a better remix quality than the baseline almost always, and the margin between baseline and proposed models is more significant as the number of sources to separation increases. The same trend can be found in the cross-database testing cases, although the overall performances drop a little due to the obvious generalization issue. There is no sensible difference between *Model-I* and *Model-II* in the table, and we will revisit this issue later in Figure 4.

There is a slight trend that the remix models favor larger contribution from the remixing regularization term controlled by ψ , as only one experiment with lowest ψ ratio, i.e., $\lambda : \psi = 1 : 1$, achieves the best remixing result out of all 13 rows of experiments. As the baseline model does not have any regularization involved, which can be seen as,

$\psi = 0$, the significant performance gap between the baseline and proposed models also showcases the merit of the proposed regularization. Note that the high standard deviation values do not imply any unstableness—they are due to the widely varying remixing weights used for testing, ranging from -24 to 24 dB.

5.2 The impact of the remixing regularization on MSS

To investigate the impact of the remix regularizer on the separation behavior, we compute the SDR, SIR and SAR of the three models' separation results using the `BSS_Eval` toolbox [25]. For this experiment, we run the models on four-source mixtures, and set $\lambda : \psi = 1 : 4$. Figure 3 summarizes the results.

Without any regularization, the baseline fails in recovering certain instruments, i.e., `piano` and `guitars` in the `Slakh` experiments, and `vocals` and `bass` in the `MUSDB` case. We observe that the performance gap mostly comes from the SAR scores, while the SIR improvement is less drastic. This signifies the neural remixers' tendency to suppress artifacts as much as possible as the source-specific artifacts do not cancel out. Meanwhile, it also shows that the proposed remixing regularization benefits general separation performance according to the SIR improvement.

5.3 The simulated user interface and the remix performance

In Figure 4, we display the relationship between the remix quality and the extent of volume control on each source in the four-source cases. Each line in the plot represents the remix SDR by adjusting the level of a target instrument from -24 to $+24$ dB, while the rest are kept unchanged. This intends to mimic the scenario where the user can adjust the volume of one instrument source by twisting a knob. The ratio between λ and ψ is set to be $1 : 4$.

The results in Figure 4 clearly show that the proposed models outperform the baseline consistently in all the remixing weight choices and in both datasets. The proposed models work significantly better when the volume control amount is nearer to 0 dB, i.e., when the intended remix

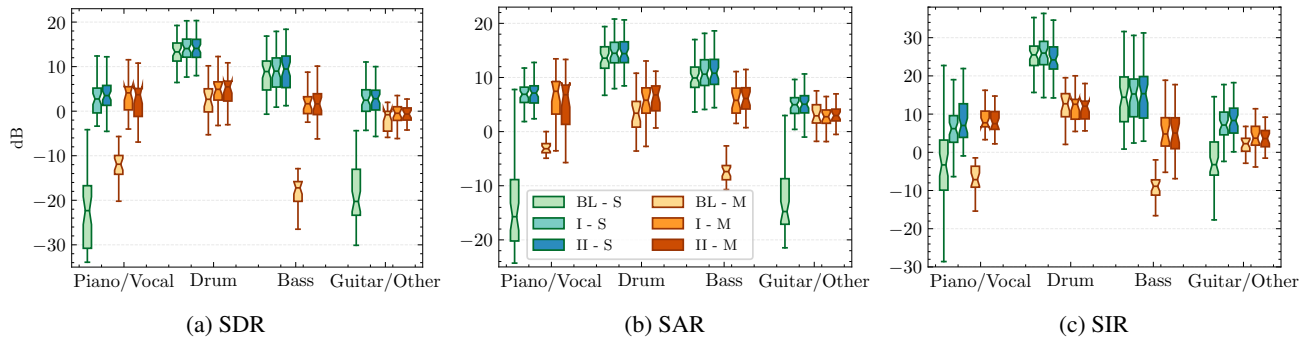


Figure 3: Source separation scores of the baseline (BS), *Model-I* (I), and *Model-II* (II) on Slakh (S) and MUSDB (M) for the four-source cases. The first and last box groups are piano and guitars in the Slakh experiments, and vocals and others in the MUSDB case.

is similar to the input mix. On the contrary, the baseline’s performance increases or decreases almost monotonically as the remix weights change. These patterns clearly show that the proposed models’ separation performance is correlated with how drastic the intended remixing weights are: if the target remix stays around the original mix, it is an easier case for the proposed models as they can effectively focus on the artifacts rather than trying to suppress interference, and vice versa. Note the difference between *Model-I* and *II* is that *Model-I* addresses this issue only during training, while *Model-II* is capable of reflecting the remixing weights to the decoding process during testing. Meanwhile, for the baseline model, the artifact and interference contained in the source estimates can be heterogeneous, making their remix stand out as distortion. Therefore, monotonic control of a source estimate can consequently monotonically influence the total remix quality. Meanwhile, both proposed models’ performance saturates when it handles the out-of-range inputs, e.g., over 12 dB.

Because of the reason stated above, the proposed models’ performance changes are more predictable—the asymmetric performance graph is common in all experiments on various instruments, datasets, and both proposed models, providing a stable user experience. The asymmetric shape is an indication of the existence of the artifact, which is boosted or suppressed together with the target source. In contrast, the baseline’s performance is less predictable. For some sources, volume amplification has a negative impact while the others suffer from a reduced volume. This observation echoes the baseline’s behavior reported in Figure 3, whose performance varies a lot over the choice of source.

It is interesting to note that, although *Model-I* does not have any inference-time mechanism to adjust the separation behavior according to the different remixing weights, it still performs on par with *Model-II*. We believe that to achieve a good sound quality for remix, it is most crucial to reduce the artifact produced in the separation step, and these two proposed models almost reach the same level in pursuing this goal. However, *Model-II* shows slightly better performance at the extreme cases around 24 dB on the Slakh dataset, which we believe is associated with its capability of utilizing remixing information during inference.

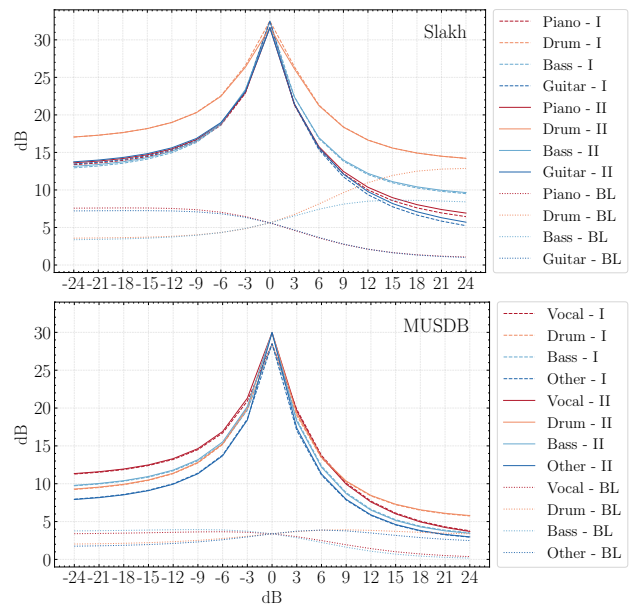


Figure 4: Remix quality with respect to volume modulator of baseline (BL), *Model-I* (I) and *Model-II* (II).

6. CONCLUSION

This paper introduced a neural remixing model to tackle the remix use case where the separated source tracks are not available. As an alternative to the conventional separator-remixer workflow, we integrated the two processes together by adding an extra regularizer to the proposed end-to-end neural remixer. We evaluated the model on two music source separation datasets, Slakh and MUSDB. Results on both datasets manifested that the regularization mechanism greatly reduces the artifact produced in the process of source separation. Therefore, our models achieved significant improvement in the remix quality. From the perspective of user interaction, we demonstrated that the relationship between the estimated remix and the intended one is reasonably correlated as opposed to that induced from the baseline model. Sound examples and source codes are available at <https://saige.sice.indiana.edu/research-projects/neural-remixer>.

7. REFERENCES

- [1] Y. Luo and N. Mesgarani, "Conv-TasNet: Surpassing ideal time–frequency magnitude masking for speech separation," *IEEE/ACM Transactions on Audio, Speech, and Language Processing*, vol. 27, no. 8, pp. 1256–1266, 2019.
- [2] J. R. Hershey, Z. Chen, J. Le Roux, and S. Watanabe, "Deep clustering: Discriminative embeddings for segmentation and separation," in *Proceedings of the IEEE International Conference on Acoustics, Speech, and Signal Processing (ICASSP)*, Mar. 2016.
- [3] E. Manilow, G. Wichern, P. Seetharaman, and J. Le Roux, "Cutting music source separation some Slakh: A dataset to study the impact of training data quality and quantity," in *Proceedings of the IEEE Workshop on Applications of Signal Processing to Audio and Acoustics (WASPAA)*. IEEE, 2019.
- [4] Z. Rafii, A. Liutkus, F.-R. Stöter, S. I. Mimilakis, and R. Bittner, "MUSDB18-HQ - an uncompressed version of MUSDB18," Aug. 2019. [Online]. Available: <https://doi.org/10.5281/zenodo.3338373>
- [5] O. Gillet and G. Richard, "Extraction and remixing of drum tracks from polyphonic music signals," in *IEEE Workshop on Applications of Signal Processing to Audio and Acoustics, 2005*. IEEE, 2005, pp. 315–318.
- [6] K. Yoshii, M. Goto, and H. Okuno, "INTER:D: a drum sound equalizer for controlling volume and timbre of drums," in *The 2nd European Workshop on the Integration of Knowledge, Semantics and Digital Media Technology, 2005. EWIMT 2005. (Ref. No. 2005/11099)*, 2005, pp. 205–212.
- [7] G. Roma, E. M. Grais, A. J. Simpson, and M. D. Plumbley, "Music remixing and upmixing using source separation," in *Proceedings of the 2nd AES Workshop on Intelligent Music Production*, 2016.
- [8] J. Pons, J. Janer, T. Rode, and W. Nogueira, "Remixing music using source separation algorithms to improve the musical experience of cochlear implant users," *The Journal of the Acoustical Society of America*, vol. 140, no. 6, pp. 4338–4349, 2016.
- [9] J. F. Woodruff, B. Pardo, and R. B. Dannenberg, "Remixing stereo music with score-informed source separation," in *Proceedings of the International Society for Music Information Retrieval Conference (ISMIR)*, 2006, pp. 314–319.
- [10] K. Itoyama, M. Goto, K. Komatani, T. Ogata, and H. G. Okuno, "Instrument equalizer for query-by-example retrieval: Improving sound source separation based on integrated harmonic and inharmonic models," in *Proceedings of the International Society for Music Information Retrieval Conference (ISMIR)*, 2008, pp. 133–138.
- [11] P. Huang, M. Kim, M. Hasegawa-Johnson, and P. Smaragdis, "Joint optimization of masks and deep recurrent neural networks for monaural source separation," *IEEE/ACM Transactions on Audio, Speech, and Language Processing*, vol. 23, no. 12, pp. 2136–2147, Dec 2015.
- [12] S. Uhlich, M. Porcu, F. Giron, M. Enenkl, T. Kemp, N. Takahashi, and Y. Mitsufuji, "Improving music source separation based on deep neural networks through data augmentation and network blending," in *2017 IEEE International Conference on Acoustics, Speech and Signal Processing (ICASSP)*. IEEE, 2017, pp. 261–265.
- [13] P. Seetharaman, G. Wichern, J. Le Roux, and B. Pardo, "Bootstrapping deep music separation from primitive auditory grouping principles," *Workshop on Self-supervision in Audio and Speech at the 37th International Conference on Machine Learning*, 2019.
- [14] P. Seetharaman, G. Wichern, S. Venkataramani, and J. Le Roux, "Class-conditional embeddings for music source separation," in *ICASSP 2019-2019 IEEE International Conference on Acoustics, Speech and Signal Processing (ICASSP)*. IEEE, 2019, pp. 301–305.
- [15] J. H. Lee, H.-S. Choi, and K. Lee, "Audio query-based music source separation," *Proceedings of the International Society for Music Information Retrieval Conference (ISMIR)*, pp. 878–885, 2019.
- [16] D. Stoller, S. Ewert, and S. Dixon, "Wave-u-net: A multi-scale neural network for end-to-end audio source separation," in *Proceedings of the International Society for Music Information Retrieval Conference (ISMIR)*, 2018.
- [17] F. Lluís, J. Pons, and X. Serra, "End-to-End Music Source Separation: Is it Possible in the Waveform Domain?" in *Proc. Interspeech 2019*, 2019, pp. 4619–4623. [Online]. Available: <http://dx.doi.org/10.21437/Interspeech.2019-1177>
- [18] A. Défossez, N. Usunier, L. Bottou, and F. Bach, "Music Source Separation in the Waveform Domain," Apr. 2021, working paper or preprint. [Online]. Available: <https://hal.archives-ouvertes.fr/hal-02379796>
- [19] J. L. Ethan Manilow, Gordon Wichern, "Hierarchical musical instrument separation," in *Proceedings of the International Society for Music Information Retrieval Conference (ISMIR)*, 2020, pp. 376–383.
- [20] G. P. Gabriel Meseguer Brocal, "Content based singing voice source separation via strong conditioning using aligned phonemes," in *Proceedings of the International Society for Music Information Retrieval Conference (ISMIR)*, 2020, pp. 819–827.
- [21] F.-R. Stöter, S. Uhlich, A. Liutkus, and Y. Mitsufuji, "Open-unmix-a reference implementation for music

source separation,” *Journal of Open Source Software*, vol. 4, no. 41, p. 1667, 2019.

- [22] H. Wierstorf, D. Ward, R. Mason, E. M. Grais, C. Hummersone, and M. D. Plumbley, “Perceptual evaluation of source separation for remixing music,” in *Audio Engineering Society Convention 143*. Audio Engineering Society, 2017.
- [23] H. Yang, K. Zhen, S. Beack, and M. Kim, “Source-aware neural speech coding for noisy speech compression,” in *Proceedings of the IEEE International Conference on Acoustics, Speech, and Signal Processing (ICASSP)*, 2021.
- [24] N. J. Bryan and G. J. Mysore, “An efficient posterior regularized latent variable model for interactive sound source separation,” in *Proceedings of the International Conference on Machine Learning (ICML)*, Atlanta, Georgia, 2013.
- [25] E. Vincent, C. Fevotte, and R. Gribonval, “Performance measurement in blind audio source separation,” *IEEE Transactions on Audio, Speech, and Language Processing*, vol. 14, no. 4, pp. 1462–1469, 2006.
- [26] M. Pariente, S. Cornell, J. Cosentino, S. Sivasankaran, E. Tzinis, J. Heitkaemper, M. Olvera, F.-R. Stöter, M. Hu, J. M. Martín-Doñas, D. Ditter, A. Frank, A. Deleforge, and E. Vincent, “Asteroid: The PyTorch-Based Audio Source Separation Toolkit for Researchers,” in *Proceedings of the Annual Conference of the International Speech Communication Association (Interspeech)*, 2020, pp. 2637–2641.
- [27] D. Yu, M. Kolbæk, Z.-H. Tan, and J. Jensen, “Permutation invariant training of deep models for speaker-independent multi-talker speech separation,” in *Proceedings of the IEEE International Conference on Acoustics, Speech, and Signal Processing (ICASSP)*. IEEE, 2017, pp. 241–245.
- [28] M. Kolbæk, D. Yu, Z.-H. Tan, and J. Jensen, “Multitalker speech separation with utterance-level permutation invariant training of deep recurrent neural networks,” *IEEE/ACM Transactions on Audio, Speech, and Language Processing*, vol. 25, no. 10, pp. 1901–1913, 2017.
- [29] D. Kingma and J. Ba, “Adam: A method for stochastic optimization,” in *Proceedings of the International Conference on Learning Representations (ICLR)*, 2015.
- [30] J. Le Roux, S. Wisdom, H. Erdogan, and J. R. Hershey, “SDR – half-baked or well done?” in *ICASSP 2019-2019 IEEE International Conference on Acoustics, Speech and Signal Processing (ICASSP)*. IEEE, 2019, pp. 626–630.